JVI Journals.ASM.org

Influence of Herpes Simplex Virus 1 Latency-Associated Transcripts on the Establishment and Maintenance of Latency in the ROSA26R Reporter Mouse Model

M. P. Nicoll, J. T. Proença, V. Connor, and S. Efstathiou

Division of Virology, Department of Pathology, University of Cambridge, Cambridge, United Kingdom

Herpes simplex virus 1 (HSV-1) can establish life-long latent infection in sensory neurons, from which periodic reactivation can occur. During latency, viral gene expression is largely restricted to the latency-associated transcripts (LATs). While not essential for any phase of latency, to date the LATs have been shown to increase the efficiency of both establishment and reactivation of latency in small-animal models. We sought to investigate the role of LAT expression in the frequency of latency establishment within the ROSA26R reporter mouse model utilizing Cre recombinase-encoding recombinant viruses harboring deletions of the core LAT promoter (LAP) region. HSV-1 LAT expression was observed to influence the number of latently infected neurons in trigeminal but not dorsal root ganglia. Furthermore, the relative frequencies of latency establishment of LAT-positive and LAT-negative viruses are influenced by the inoculum dose following infection of the mouse whisker pads. Finally, analysis of the infected cell population at two latent time points revealed a relative loss of latently infected cells in the absence of LAT expression. We conclude that the HSV-1 LATs facilitate the long-term stability of the latent cell population within the infected host and that interpretation of LAT establishment phenotypes is influenced by infection methodology.

Herpes simplex virus 1 (HSV-1) is a ubiquitous human pathogen responsible for a number of important diseases, ranging from recurrent oral and genital ulceration to viral keratitis, encephalitis, and disseminated infection of neonates. During lytic replication, >80 genes are expressed from the virus genome in an extensive transcription cascade, but in stark contrast, the latent transcription program is largely restricted to a single 8.3-kb transcript termed the latency-associated transcript (LAT) located within the repeats flanking the unique-long (U_L) region of the virus genome (25, 31, 41, 46). The majority of data with regard to LAT function have been elucidated from studies using small-animal models of HSV-1 infection. These models have shown that the LATs are not essential for the establishment or maintenance of infection or for reactivation from latency (15, 36, 40). Despite this, LAT-null mutants have been reported to reactivate with reduced efficiency in rabbit models of spontaneous reactivation (28) and induced reactivation (12) as well as in mouse ganglia explanted or induced to reactivate *in vivo* (21, 35, 44). On the basis of the utilization of contextual analysis of DNA (CXA-D) to enumerate viral DNA-positive cells, it has been proposed that this deficiency is the result of a reduced capacity for latency establishment, suggesting that the LATs function during entry into latency, rather than directly during reactivation (44). Importantly, this study was able to quantify the frequency of HSV genome-positive cells during latency, and by increasing the latent burden of LAT-null virus to wild-type virus levels, the reactivation deficit of the LAT-deficient mutant was reversed (43). Nonetheless, other studies have concluded that LAT-negative HSV-1 and -2 mutants reactivate with reduced efficiency even when total virus DNA loads during latency approach wild-type levels (12, 13, 21). In addition, a number of studies have demonstrated the stability of wild-type latent viral DNA loads over time (9, 11), and an additional study demonstrated no role for LATs in latency maintenance (36). However, with the appreciation that the number of HSV genomes per latent neuron can range between <10 and >1,000 copies (32), measurements of total HSV DNA loads during latency may not provide an accurate reflection of the number of infected neurons. Given these uncertainties, it remains unclear whether the LATs function during establishment and/or reactivation and whether they have additional functions involved in the maintenance of latent infection.

We have previously described the ROSA26R reporter mouse model of infection allowing historical marking of neuron infection via the use of HSV-1 strain SC16 recombinants expressing Cre recombinase (29). In this study, we used this system to investigate both latency establishment and long-term stability by generating mutants lacking the core LAT promoter (LAP). These viruses were shown to be capable of establishing latency at a greater frequency than LAT promoter-positive HSV-1, but this phenotype was sensitive to the input virus dose. Furthermore, results of comparisons of marked-cell numbers 30 days postinfection (d.p.i.) and >110 d.p.i. suggest that the latent cell reservoir is less stable in the absence of LAT expression.

MATERIALS AND METHODS

Cells and viruses. All viruses were derived from HSV-1 strain SC16 (12a). Baby hamster kidney (BHK) cells were utilized for virus stock production and plaque assays, unless otherwise stated, and were maintained in complete Dulbecco's modified Eagle's medium (DMEM) containing 10% fetal calf serum (FCS), 10% tryptose phosphate broth, 2 mM L-glutamine, penicillin (100 U/ml), and streptomycin (100 μg/ml).

MRC-5 cells utilized for explant reactivation assays were maintained with complete DMEM, additionally supplemented with am-

Received 14 March 2012 Accepted 6 June 2012
Published ahead of print 13 June 2012
Address correspondence to S. Efstathiou, se@mole.bio.cam.ac.uk.

doi:10.1128/JVI.00652-12
The authors have paid a fee to allow immediate free access to this article.

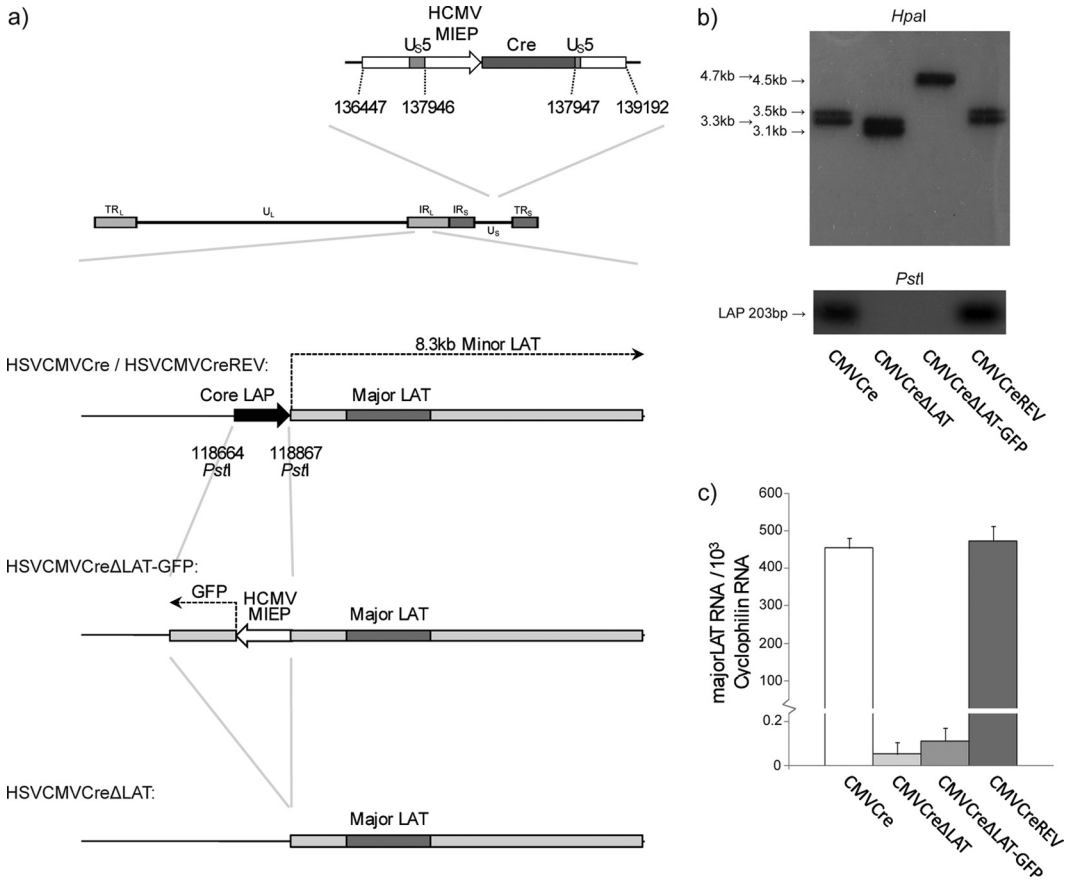

FIG 1 Generation of Cre reporter viruses bearing deletions of the core LAT promoter. (a) Genomic structures of HSV CMVCre, HSV CMVCreΔLAT, HSV CMVCreΔLAT-GFP, and HSV CMVCreREV. All four viruses harbor an HCMV MIEP-Cre recombinase expression cassette within the nonessential HSV-1 U_S5 locus. (b) Genomic structures as analyzed by Southern blot hybridization. Restriction digest with HpaI demonstrates all predicted restriction fragments. Deletion of the core LAT promoter within HSV CMVCreΔLAT and HSV CMVCreΔLAT-GFP as well as its rescue within HSV CMVCreREV was confirmed by PstI restriction digest. The 3.3-kb HpaI fragment encoded within pPSTD1 was utilized as a radiolabeled probe. (c) LAT expression was quantified by qRT-PCR from total RNA extracted from TG latently infected with all four viruses, utilizing primers for major LAT and cyclophilin RNA. Histograms represent the mean (± SEM) numbers of major LAT RNA copies per 10^3 copies of cyclophilin RNA from triplicate PCRs.

photericin B (Fungizone; 2.5 μg/ml) and 1× nonessential amino acids (PAA) for long-term culture.

Plasmids. All HSV-1 genetic coordinates used throughout this study were determined on the basis of a sequence available at GenBank (accession number NC_001806) (24).

pPSTD1 (2) comprises a 3.3-kb HpaI fragment of HSV-1 strain SC16 (HSV-1 nucleotides [nt] 117010 to 120301), containing the HSV-1 LAT promoter.

pPSTDΔLAT was constructed by the removal of the 203-bp PstI fragment (HSV-1 nt 118664 to 118867) from pPSTD1. The 203-bp PstI fragment corresponds to the HSV-1 core LAP element at −142 to +61 bp relative to the minor LAT transcription start site (nt 118803) (38).

pPSTDΔLAT-CMVGFP was derived from pPSTD1 and contains a 1,369-bp NsiI-PstI fragment derived from pcDNA3 (Invitrogen) encoding green fluorescent protein (GFP) under the control of the human cytomegalovirus (HCMV) major immediate early promoter (MIEP) in place of the 203-bp PstI core LAP. GFP is transcribed by the HCMV MIEP in the opposite orientation to the LAT locus.

Construction and characterization of recombinant viruses. HSV CMVCreΔLAT-GFP was constructed by cotransfecting pPSTDΔLAT-CMVGFP linearized with BamHI and HSV CMVCre (29)-infected cell DNA to produce a virus in which the 203-bp core LAP sequence was replaced by the HCMV MIEP GFP cassette in both Repeat-Long (R_L) genomic regions. GFP is transcribed by the HCMV MIEP in the opposite orientation to the LAT locus.

HSV CMVCreREV was constructed by cotransfecting pPSTD1 linearized with BamHI and HSV CMVCreΔLAT-GFP-infected cell DNA to produce a GFP-negative virus restored for the core LAP in both R_L genomic regions.

HSV CMVCreΔLAT was constructed by cotransfecting pPSTDΔLAT linearized with BamHI and HSV CMVCreΔLAT-GFP-infected cell DNA to produce a GFP-negative virus retaining the 203-bp LAP sequence deletion in both R_L genomic regions.

All virus recombinants were isolated and plaque purified by limiting dilution. Viral genomic structures were confirmed by restriction endonuclease digestion and Southern blot hybridization (Fig. 1b).

In vitro growth curve analyses were performed by infecting monolayers of BHK cells with 0.01 PFU/cell. Cells were incubated for 1 h, and extracellular virus was inactivated with citric acid solution (135 mM NaCl, 10 mM KCl, 40 mM citric acid). Infected cell monolayers were sampled at set time points over a 72-h period and stored at −70°C prior to assay.

In vivo growth curves utilized female BALB/c mice (Harlan, United Kingdom) at 8 weeks of age. All infections were conducted using isofluorane anesthesia. Ear pinna infections were conducted by pipetting 20 μl of virus inoculum containing 2×10^6 PFU onto the left ear

pinna. Light scarification (20 shallow scratches) with a 27-gauge needle was then applied to the ear pinna through the inoculum. Mice were killed by CO_2 asphyxiation, and the inoculated ear and ipsilateral CII, CIII, and CIV dorsal root ganglia (DRG) were dissected into complete DMEM for viral titration following storage at −70°C. Samples were freeze-thawed, homogenized, and freeze-thawed once more prior to assay. Whisker pad inoculation was conducted via the same methodology, except that animals were infected by scarification of both whisker pads by the use of 40 μl of viral inoculum harboring 10^6 PFU. Mice were killed by CO_2 asphyxiation, and whisker pads and trigeminal ganglia (TG) and brain tissue were dissected into complete DMEM for viral titration following storage at −70°C. Samples were freeze-thawed, homogenized, and freeze-thawed once more prior to assay.

ROSA26R reporter mice (39) were used for the *in vivo* characterization of HSV recombinants encoding Cre recombinase as previously described (29, 30). Groups of adult mice (>8 weeks of age) that differed in age by less than 2 weeks were infected upon the ear pinna or whisker pads. Mice were killed by CO_2 asphyxiation at various times postinfection, and the ipsilateral CII, CIII, and CIV DRG (following ear infection) or both TG (following whisker pad infection) were dissected, pooled, and fixed on ice for 1 h in 4% paraformaldehyde–phosphate-buffered saline (PBS) and incubated in X-Gal (5-bromo-4-chloro-3-indolyl-β-D-galactopyranoside) as described previously (20). Marked-cell counts to determine potential differences between virus groups were performed in a blinded manner to avoid experimental bias. This study predominantly utilized male mice. Where that was not possible, groups of equal numbers of males and females were used but were divided evenly between LAT-positive and LAT-negative mutants. The sex of the ROSA26R mice did not affect the phenotypes described in this study (data not shown).

All animal experiments were performed under United Kingdom Home Office Project License 80/2205.

DNA extractions for real-time quantitative PCR (qPCR) were performed on individual TG or pooled CII, CIII, and CIV DRG from five mice. The ganglia were homogenized and incubated in 0.5% sodium dodecyl sulfate (SDS) and 50 g of proteinase K/ml in TE buffer (10 mM Tris HCl, 1 mM EDTA [pH 8]) overnight at 37°C. Samples were sonicated, and phenol chloroform was extracted before purification with Qiagen PCR purification columns. qPCRs were conducted as previously described (7). Virus genome was quantified with ICP0 promoter-specific primers, and adenine phosphoribosyltransferase (APRT) was utilized as a cellular DNA control. PCRs were run as duplex reactions. The ICP0 promoter forward primer was GGAAAGGCGTGGGGTATAA, the reverse primer was AAC GTAGGCGGGGCTTC, and the TaqMan probe was TCGCATTTGCAC CTCGGCAC. The APRT forward primer was GGGGCAAAACCAAAAA AGGA, the reverse primer was TGTGTGTGGGGCCTGAGTC, and the TaqMan probe was TGCCTAAACACAAGCATCCCTACCTCAA (8). PCR products were quantified using a Corbett Research Rotor-Gene and associated software as the copy numbers per PCR, calculated from triplicate results from each PCR. A standard curve for each gene region was generated using dilutions of appropriate plasmids. Reaction conditions utilized were 15 min at 95°C, with 45 cycles of 15 s at 95°C and 60 s at 60°C.

LAT RNA expression was assessed from pooled TG from five latently infected mice per virus. Ganglia were removed into 1 ml of RNAlater (Qiagen), prior to RNA extraction. Total RNA was extracted and DNase I treated from pooled TG by the use of TRIzol reagent and a PureLink RNA minikit (Invitrogen). RNA was reverse transcribed (RT) with a TaqMan MicroRNA reverse transcription kit (Invitrogen), according to the manufacturer's protocol. RT reactions were primed with random primers (Invitrogen) at a concentration of 0.2 μg μl^{-1}. qPCRs of samples and RT-negative controls were conducted with the aforementioned reaction conditions utilized for DNA load quantification, utilizing primers for mouse cyclophilin and major LAT RNA. The LAT forward primer was CCAGGCAGTAAGACCCAAGC, the reverse primer was GGCCGGTGT CGCTGTAAC, and the TaqMan probe was TCCCACCCCGCCTGTGTT TTT. The cyclophilin forward primer was GTCTCCTTCGAGCTGTT TGC, the reverse primer was GAGGAACCCTTATAGCCAAATCC, and the TaqMan probe was ACAAAGTTCCAAAGACAGCAGAAAACTTTC.

Whole-ganglion preparation and immunohistochemistry for HSV-1 antigen detection during latency was performed as described by Sawtell (33). However, antigen detection was conducted with anti-HSV-1 rabbit polyclonal (Dako) and horseradish peroxidase (HRP)-conjugated donkey anti-rabbit (Amersham Biosciences) antibodies. Staining was developed with a 3,3′-diaminobenzidine (DAB) peroxidase substrate kit (Vector Laboratories). Detection of antigen-positive cells was determined alongside naive and acutely infected tissue as negative and positive controls, respectively. All counts to determine potential differences between virus groups were performed on blinded material to avoid experimental bias.

Statistical analysis of ROSA26R mouse ganglion marked-cell populations was conducted using the Mann-Whitney U and Kruskal-Wallis tests for paired- and multiple-group analyses, respectively.

RESULTS

***In vitro* and *in vivo* characterization of HSV-1 recombinants deleted for the core LAT promoter.** Cre recombinase-expressing viruses carrying deletions of the LAP with or without an HCMV MIEP GFP expression cassette as well as a LAP revertant virus were constructed on the HSV-1 SC16 genomic background as described in Materials and Methods. The predicted structures of these viruses are represented in Fig. 1a and were confirmed by Southern blot hybridization (Fig. 1b) using the purified 3.3-kb HpaI DNA fragment from pPSTD1 as a probe. Wild-type 3.3-kb and 3.5-kb HpaI restriction fragments (from the IR_L and TR_L, respectively) and the core LAP 203-bp PstI restriction fragment were detected from both HSV CMVCre and HSV CMVCreREV digests. Both HSV CMVCreΔLAT and HSV CMVCreΔLAT-GFP were negative for the core LAP 203-bp PstI fragment. Detection of 4.5-kb and 4.7-kb HpaI restriction fragments confirmed the insertion of the HCMV MIEP GFP expression cassette in both the IR_L and the TR_L genome regions of HSV CMVCreΔLAT-GFP (Fig. 1b). Quantitative reverse transcriptase PCR (qRT-PCR) analysis of RNA recovered from trigeminal ganglia (TG) of mice latently infected with both ΔLAT mutants (HSV CMVCreΔLAT and HSV CMVCreΔLAT-GFP) demonstrated a 4,000-to-8,000-fold ablation of major LAT expression in comparison to either HSV CMVCre or the HSV CMVCreΔLAT-GFP-revertant virus designated HSV CMVCreREV (Fig. 1c). Low-multiplicity-of-infection (low-MOI) growth curves demonstrated that the *in vitro* replication kinetics of all recombinants were highly similar (Fig. 2a). Acute replication kinetics were assessed *in vivo* utilizing the mouse ear pinna infection model. Assessment of infectious virus titers at 3, 5, and 7 d.p.i. showed that replication results for all recombinants in both ears (Fig. 2b) and in pooled CII, CIII, and CIV dorsal root ganglia (DRG) were similar (Fig. 2c). All viruses displayed equivalent levels of latency establishment within BALB/c DRG in comparison to the previously characterized Cre-expressing recombinant SC16 strain HSV CMVCre (29) as observed by real-time PCR quantification of latent viral DNA loads from pooled CII, CIII, and CIV DRG dissected 70 d.p.i. (Fig. 2d). In addition, explant reactivation analysis demonstrated that all viruses were reactivation competent and generated similar amounts of virus following 5 days of culture of DRGs dissected 40 d.p.i. (Fig. 2e). Acute-phase replication kinetics were also determined following whisker pad infection with HSV CMVCre, HSV CMVCreΔLAT-GFP, and HSV CMVCreREV. Titers achieved within the periphery, TG, and brain tissue were similar for all viruses in BALB/c mice (Fig. 2f to

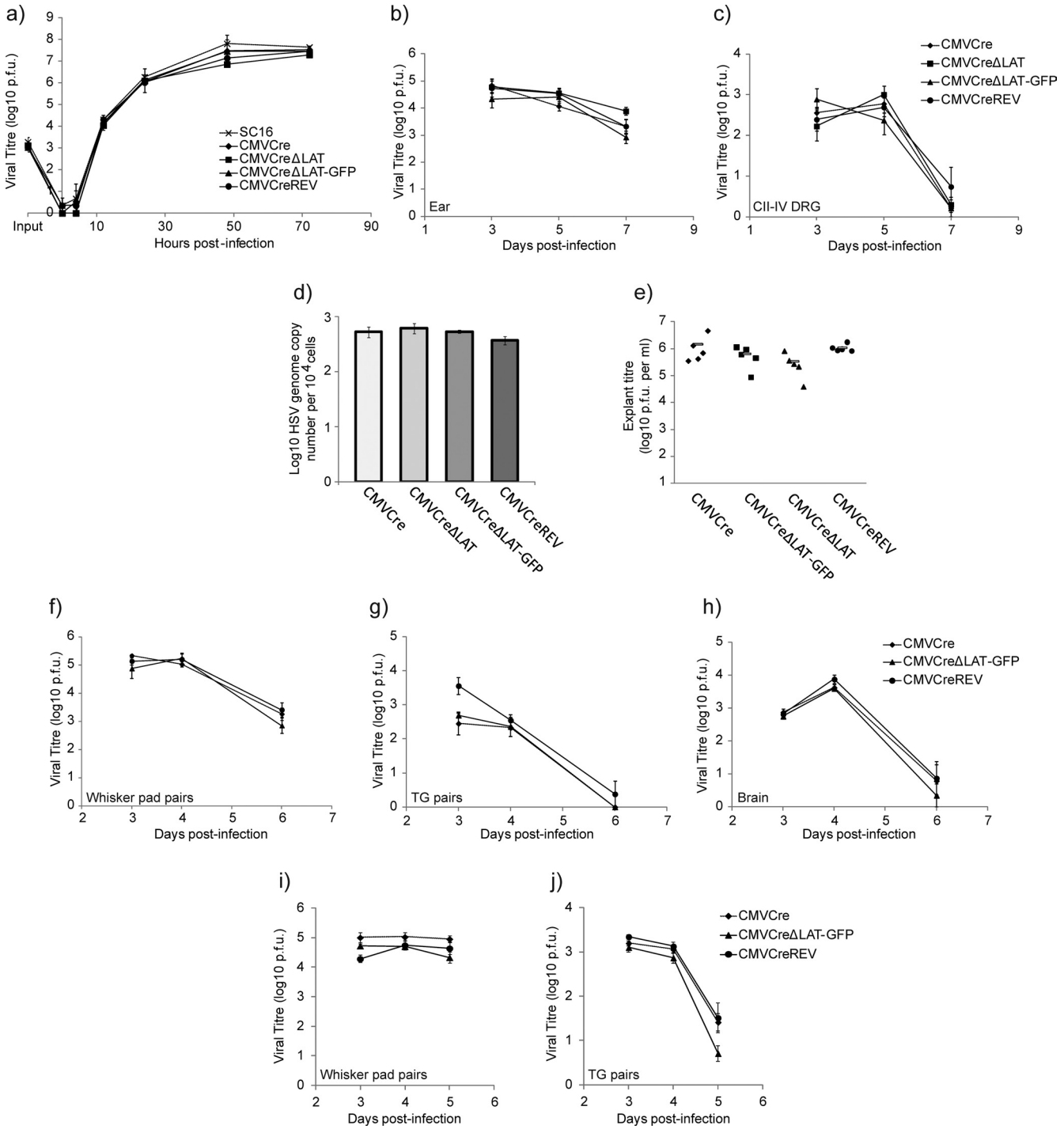

FIG 2 Cre reporter virus growth characterization. (a) Low (0.01) MOI. *In vitro* growth curves of recombinant viruses and wild-type strain SC16 from duplicate experiments performed in BHK cells are shown. (b and c) *In vivo* replication of recombinant viruses in the ears (b) and pooled CII, CIII, and CIV DRG (c) 3, 5, and 7 d.p.i. following inoculation of BALB/c mice on the left ear with 2×10^6 PFU. Data points represent mean (± SEM) viral titers from five mice at each time point. (d) Virus latent DNA loads. qPCR was performed on DNA extracted from pooled CII, CIII, and CIV DRG from five latently infected mice, utilizing primers for the ICP0 promoter and cellular APRT. Values represent mean (± SEM) numbers of HSV genome copies per 10^4 copies of APRT from triplicate PCRs. (e) Explant reactivation competence of HSV recombinants. CII, CIII, and CIV ganglia from latently infected mice were cultured for 5 days and assayed for reactivating virus. Each point represents viral titers detected per mouse, and the bars represent the averages of these data. (f to h) *In vivo* replication of recombinant viruses in both whisker pads (f), TG pairs (g), and brain (h) 3, 4, and 6 d.p.i. following inoculation of BALB/c mice on both whisker pads. Data points represent mean (± SEM) viral titers from five mice at each time point. (i and j) *In vivo* replication of recombinant viruses in both whisker pads (i) and TG pairs (j) 3, 4, and 5 d.p.i. following inoculation of ROSA26R mice on both whisker pads with 10^6 PFU. Data points represent mean (± SEM) viral titers from five mice at each time point. No mortality was observed in any of the above-described experiments.

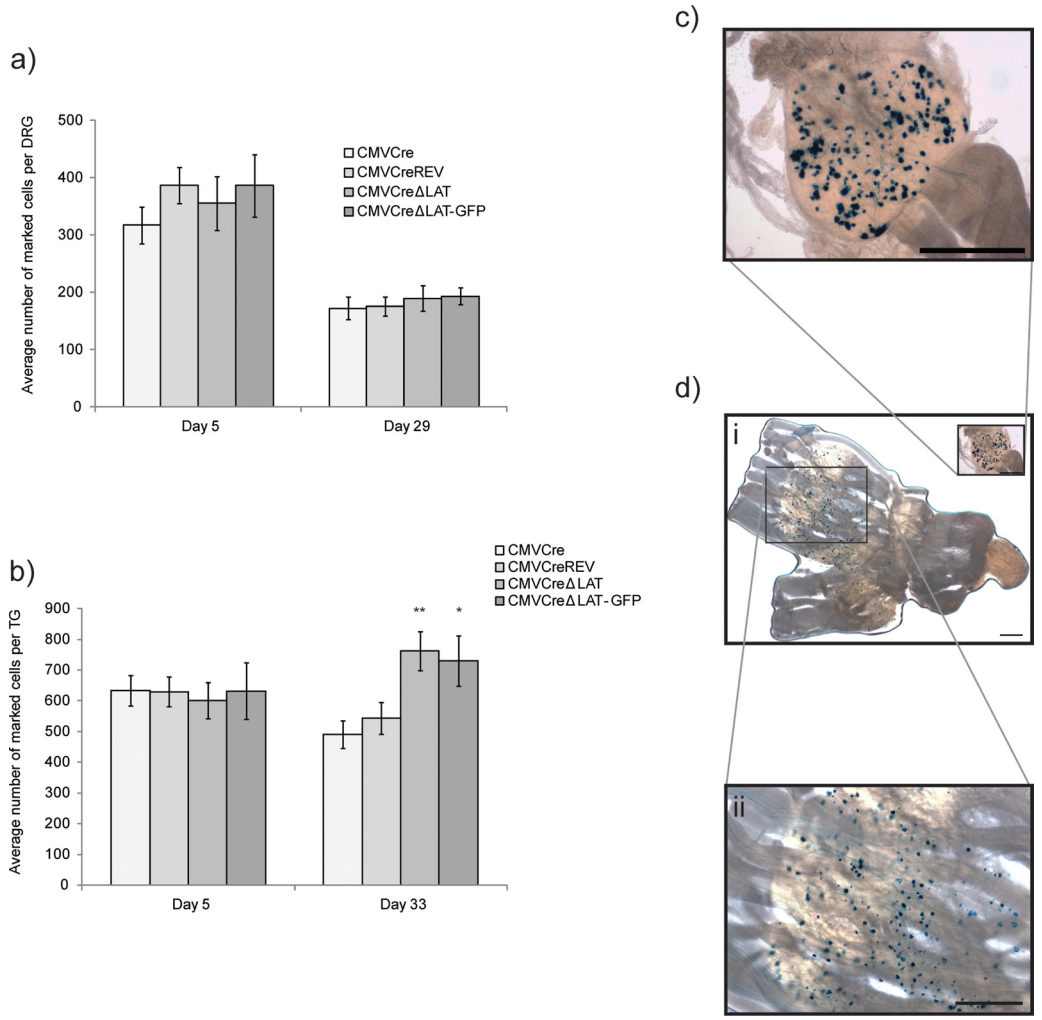

FIG 3 LAT promoter-negative HSV-1 establishes latency at a higher frequency than the wild type in the TG. (a and b) Detection of Cre-marked cells following infection of ROSA26R mice with HSV CMVCre, HSV CMVCreΔLAT, HSV CMVCreΔLAT-GFP, and HSV CMVCreREV in the DRG (a) and TG (b). Histograms represent the mean (± SEM) numbers of positive cells per ganglion detected at the specified time points postinfection. *P* values of 0.005 and 0.058 are represented by ** and *, respectively. (c and d) Light micrographs of latently infected DRG (c) and TG (d, panels i and ii). Bars, 1 mm. A single HSV CMVCre-infected mouse was euthanized following whisker pad infection when pathology reached a predetermined threshold of severity. No other mortality was recorded.

h), as well as in the periphery and TG of ROSA26R reporter mice (Fig. 2i and j). Using these assays, we conclude that LAT-positive and LAT-negative HSV-1 recombinants replicate in similar manners both *in vitro* and *in vivo*. Furthermore, these assays revealed that LAT-positive and LAT-negative recombinant viruses both establish and reactivate from latency within the DRGs in comparable manners.

Latency establishment is enhanced in the absence of LAT expression within the trigeminal ganglion. It has been reported that a major phenotype observed with LAT-deficient mutants is that of a reduced efficiency for reactivation (12, 21, 28, 35), and there is evidence to indicate that the reactivation deficit observed with LAT mutants can be explained by a decrease in the efficiency of latency establishment (42, 44). Whether LATs have a dedicated function in promoting reactivation is less clear, although recently it has been proposed that LATs function to maintain the *in vivo* reactivation competence of HSV-1 following repeated hyperthermic stress (43).

We sought to investigate whether disparities existed between the numbers of infected cells in which HSV-1 enters latency in the presence and absence of LAT expression by utilizing the ROSA26R reporter mouse model of HSV-1 latency (29, 30). In this model, expression of Cre recombinase from the virus leads to excision of a *loxP*-flanked neomycin resistance gene cassette situated between the constitutive ROSA26 promoter and downstream *lacZ* reporter gene within the infected cell. As a result, *lacZ* is constitutively expressed from the cell genome. Thus, infection of mice with HSV-1 encoding Cre recombinase under the control of the HCMV MIEP results in the permanent genetic marking of latently infected neurons that can be visualized and accurately quantified following incubation with X-Gal (29, 30, 47).

Forty ROSA26R mice were inoculated on the left ear with 10^6 PFU of HSV CMVCre, HSV CMVCreΔLAT, HSV CMVCreΔLAT-GFP, or HSV CMVCreREV in groups of 10 and sampled at 5 and 29 d.p.i. (Fig. 3a). CII, III, and IV DRG were dissected and fixed, and following incubation with X-Gal, the numbers of reporter gene-

positive cells were enumerated (Fig. 3a and c). During acute infection, at 5 d.p.i., the average numbers of marked cells per ganglion were similar across all experimental groups: 317.2 ± 32.4, 355.4 ± 47.1, 386.6 ± 54.4, and 387.1 ± 31.3 positive cells per ganglion (± standard errors of the means [SEM]) for HSV CMVCre, HSV CMVCreΔLAT, HSV CMVCreΔLAT-GFP, and HSV CMVCreREV, respectively (*P* for comparisons to HSV CMVCre results = 0.77, 0.34, and 0.15 for HSV CMVCreΔLAT, HSV CMVCreΔLAT-GFP, and HSV CMVCreREV, respectively). Consistent with previous reports (29, 30), a decrease in the numbers of marked cells was observed in the transition from acute to latent infection (day 29 p.i.) and, as observed for the day 5 acute-infection time point, the average numbers of marked cells per ganglion were similar across all experimental groups: 158.7 ± 19.8, 189.8 ± 22.5, 193.1 ± 15.0, and 175.3 ± 16.4 positive cells per ganglion (± SEM) for HSV CMVCre, HSV CMVCreΔLAT, HSV CMVCreΔLAT-GFP, and HSV CMVCreREV, respectively (Fig. 3a) (*P* for comparisons to HSV CMVCre results = 0.44, 0.32, and 0.65 for HSV CMVCreΔLAT, HSV CMVCreΔLAT-GFP, and HSV CMVCreREV, respectively). These results are consistent with the equivalent virus DNA loads detected during latency (Fig. 2d) and together suggest that LAT expression does not affect latency establishment in the DRG.

It has been previously shown that establishment and reactivation phenotypes of LAT-deficient mutants show a strong anatomical dependence on the TG but not DRG (35). To investigate whether establishment deficits could be detected in TG of reporter animals, 55 ROSA26R mice were infected via scarification of the whisker pads with HSV CMVCre, HSV CMVCreΔLAT, HSV CMVCreΔLAT-GFP, or HSV CMVCreREV in groups of 15 animals (or groups of 10 animals, for HSV CMVCreΔLAT-GFP). TG were removed from five mice per group at 5, 33, and 110 d.p.i. and individually analyzed for marked cells (Fig. 3d, panels i and ii). During acute infection (5 d.p.i.), the average numbers of marked cells per ganglion were once again highly similar across all experimental groups, though at 2-fold-higher numbers than were observed in DRG: 633.5 ± 49.2, 601.1 ± 58.8, 631.6 ± 103.0, and 629.5 ± 48.7 marked cells per ganglion (± SEM) for HSV CMVCre, HSV CMVCreΔLAT, HSV CMVCreΔLAT-GFP, and HSV CMVCreREV, respectively (Fig. 3b) (*P* for comparisons to HSV CMVCre results = 0.73, 0.96, and 0.79 for HSV CMVCreΔLAT, HSV CMVCreΔLAT-GFP, and HSV CMVCreREV, respectively). During latency (33 d.p.i.), both HSV CMVCre and HSV CMVCreREV marked-cell populations had decreased by an average of 19%, to 489.7 ± 45.0 and 542.5 ± 52.0, respectively. In contrast, we observed that both ΔLAT virus infections led to an average increase in the numbers of marked cells during the transition from acute infection (day 5 p.i.) to latent infection (day 33 p.i.) (Fig. 3b), with 762.4 ± 63.5 and 729.7 ± 81.1 marked cells per ganglion (± SEM) detected for HSV CMVCreΔLAT and HSV CMVCreΔLAT-GFP, respectively, at the latter time point. This divergence of marked-cell populations at 33 d.p.i. was significant: $P = 0.0058$ and 0.0587 (compared to HSV CMVCre) and 0.0172 and 0.0376 (compared to HSV CMVCreREV) for HSV CMVCreΔLAT and HSV CMVCreΔLAT-GFP, respectively. These data show that, following whisker pad infection of ROSA26R reporter mice, two HSV-1 recombinants deficient for LAT expression establish latency in the TG at a higher frequency than both parental and revertant viruses that are wild type for the LAT promoter locus.

LAT expression does not influence the average DNA copy number per infected cell. It has been shown previously that HSV-1 genome copy numbers per infected cell during latency are highly variable, ranging from one to >1,000 copies (32). Within this study, the majority of infected neurons possessed 1 to 10 or 10 to 100 HSV-1 genome copies at a range of inoculum doses. LATs have been shown to suppress lytic gene expression and replication in mouse neurons and neuronal cell lines (10, 22) and to encode microRNAs (miRNAs) that can suppress translation of the key IE gene products ICP0 and ICP4 in an *in vitro* model system (45). It has been hypothesized that LAT expression may resist the entry of HSV-1 into lytic replication following infection with high numbers of virus particles (42). If that hypothesis is correct, in the absence of LAT expression a greater proportion of neurons infected with high HSV-1 genome loads would die, eventually resulting in a population of latent neurons that would, on average, possess fewer genome copies per cell than observed with wild-type HSV-1. Of importance, the HSV-1 genome copy number per neuron appears to positively correlate with the reactivation competence of different HSV-1 strains (34) and may thus represent an important determinant of recrudescence. In order to determine whether expression of LATs influences the average latent genome copy number per cell, 26 mice were infected via the whisker pads with 10^6 PFU of either HSV CMVCreΔLAT-GFP or HSV CMVCreREV in groups of 13. At 30 d.p.i., DNA was extracted from individual TG for HSV-1 genome quantification ($n = 14$) and the other 12 TG from each virus-infected group were fixed for X-Gal incubation and quantification of marked-cell numbers. In the latter procedure, HSV CMVCreΔLAT-GFP and HSV CMVCreREV possessed an average of 595.25 ± 38.68 and 444.5 ± 17.61 marked cells per TG (± SEM), respectively ($P = 0.0032$). For each virus-infected group, total HSV-1 genome copies for each TG were divided by these data to obtain an estimate for the average genome copy number per marked cell. We calculated average genome copy numbers per marked cell ± SEM of 90.0 ± 19.6 and 94.5 ± 17.4 for HSV CMVCreΔLAT-GFP and HSV CMVCreREV viruses, respectively. These data suggest that, following inoculation with 10^6 PFU (a dose at which LAT-negative mutants establish latency at a greater frequency than wild-type virus), LAT expression does not influence the average genome copy number during the establishment of latency in the mouse.

Absence of LAT expression is not associated with a reactivation deficit in the ROSA26R mouse. Assessment of reactivation competence during initial characterization of latent DRG infection demonstrated that all of the viruses were competent for reactivation during explant culture (Fig. 2e). To differentiate the kinetics of virus recovery, ROSA26R mice were infected via the whisker pad and, 49 d.p.i., individual latently infected TG were cut into five equally sized pieces and cultured on MRC-5 monolayers. When cytopathic effect (CPE) was observed in these monolayers, the ganglion was scored positive for reactivation. Utilizing this system, we observed no gross deficit in reactivation kinetics in comparisons of LAT-positive and -negative viruses (Fig. 4a). All recovered viruses were identified as representing the correct input via PCR utilizing primers flanking the core LAT promoter (Fig. 4b and c).

The capacity of LAT-negative virus to establish latency with increased efficiency in the TG is lost with increasing virus inoculum. Due to the observed differences between DRG and TG infection models in latency establishment, we next sought to determine whether our observations were the result of ganglion-specific differences or methodological differences in our infection procedures. ROSA26R mice were inoculated with 10^5, 10^7, and

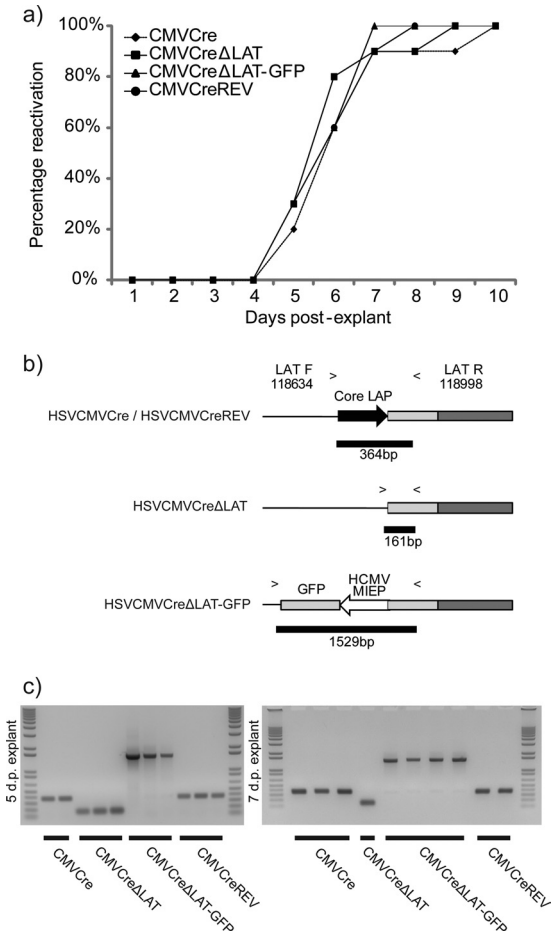

FIG 4 Explant reactivation kinetics are unimpaired in the absence of LAT expression following latency in the TG. (a) ROSA26R mice were inoculated with 10^6 PFU of each recombinant virus per whisker pad. At 40 d.p.i., TG were dissected ($n = 10$ per recombinant), cut into five pieces, and plated onto MRC-5 cell monolayers, with pieces from one whole TG per dish. Plates were scored positive for reactivation upon observation of CPE within monolayers. (b) PCR with primers flanking the LAT region was designed to identify each recombinant. (c) Reactivating virus identity was successfully confirmed by PCR. The identities of viruses reactivating 5 and 7 days postexplant are shown. No mortality was recorded within this experiment.

6×10^7 PFU of either HSV CMVCreΔLAT-GFP or the revertant HSV CMVCreREV on both whisker pads. At time points during latency (~30 d.p.i.), mice were killed and both TG dissected for marked-cell enumeration. The number of TG analyzed, the d.p.i. of dissection, and the average marked-cell numbers for all infection doses are presented in Table 1. Following infection with 10^5 PFU, we noted that latent HSV CMVCreREV-infected cell numbers were once again lower than those seen with the ΔLAT mutant but that this time they were lower by ~50%, a markedly increased difference from previous 10^6 PFU infections. In contrast, when inoculum doses were increased to 10^7 PFU and beyond, this trend was reversed, with HSV CMVCreΔLAT-GFP infections now resulting in fewer latently infected cells than HSV CMVCreREV infections (Fig. 5a).

In the light of this dose dependence of latency establishment within the TG, we reevaluated the possibility that these differences were tissue specific by infecting ROSA26R mice with HSV CMVCreΔLAT-GFP or HSV CMVCreREV via the ear route of infection at doses of 10^5 and 10^7 PFU. At 30 d.p.i., mice were killed and CII, III, and IV DRG dissected for marked-cell enumeration. We observed no significant difference between the frequencies of latency establishment of the two viruses at either dose, with average numbers of marked cells per DRG ± SEM of 160.8 ± 13.7 and 150.4 ± 18.7 at the 10^5 PFU dose and 189.1 ± 16.0 and 174.0 ± 16.9 at the 10^7 PFU dose for HSV CMVCreΔLAT-GFP and HSV CMVCreREV, respectively (Fig. 5b).

Together, these dosage data suggest that the effect of LAT expression on HSV-1 latency establishment is anatomically localized to the TG.

The maintenance of HSV-1 latency is impaired in the absence of LAT expression. Experimental infection of ROSA26R reporter mice with wild-type and LAT-negative HSV-1 recombinants demonstrates that the frequency of latency establishment in TG can be enhanced, with no effect upon the average DNA copy number. Additionally, we have shown that in the absence of LAT expression, the frequency of establishment of HSV-1 latency is sensitive to increasing concentrations of viral inoculum. Next, we assessed the long-term stability of cell marking during experimental infection of the ROSA26R mouse TG. In three independent experiments, mice were infected with 10^6 PFU on both whisker pads and ganglia were dissected and incubated in X-Gal at latent (29 to 33 d.p.i.) and "late-latent" (110 to 140 d.p.i) time points. The viral recombinants tested, numbers of TG analyzed, d.p.i. of dissection, and average marked-cell numbers at each time point are presented in Table 2. The average numbers of marked cells at either time point were utilized to estimate the rate of change over the duration of infection. An assumption was made that the rate of change in cell numbers was constant over time. In agreement with published observations, viruses that were wild type for the LAT promoter demonstrated a relatively stable population of marked cells between the early and late time points during latency (29), with HSV CMVCre and HSV CMVCreREV losing averages of 0.24 and 0.07 ± 0.56 (SEM) marked cells per TG per day, respectively (Fig. 6a). In contrast, both HSV CMVCreΔLAT-GFP and HSV CMVCreΔLAT exhibited a loss of marked cells between 29 and 33 d.p.i. and 110 and 140 d.p.i., with the two mutants losing an average of 1.72 and 1.63 ± 0.6 (SEM) marked cells, respectively, per

TABLE 1 Summary of individual experiment data from inoculum dosage study

Dose (PFU)[a]	Avg (range) no. of marked cells per TG: HSV CMVCreΔLAT-GFP	HSV CMVCreREV	% difference (LAT^+ vs LAT^-)	P^b	n^c	Day p.i.[d]
10^5	282.1 (0–825)	92.9 (0–245)	67.1	0.0340	10	42
	402.2 (213–475)	248.7 (47–446)	38.2	0.0062	10	36
10^6	729.7 (270–1,105)	542.5 (334–840)	25.7	0.0380	10	33
	715.0 (219–1,022)	564.0 (321–935)	21.1	0.2700	10	30
	595.3 (385–850)	444.5 (318–541)	25.3	0.0032	12	30
	595.0 (271–1,009)	423.3 (213–617)	28.9	0.0017	18	29
10^7	387.7 (246–521)	488.0 (371–646)	−25.9	0.1400	10	35
6×10^7	533.1 (321–791)	645.5 (439–833)	−21.1	0.0120	20	30

[a] At the 10^6 PFU dose, a single HSV CMVCreΔLAT-GFP-infected mouse was killed when pathology reached a predetermined threshold of severity. No mortality was recorded at any other dose.
[b] *P* values obtained using Mann-Whitney U test.
[c] Numbers of ganglia enumerated per virus-infected group.
[d] Numbers of days postinfection that TG were dissected for analysis.

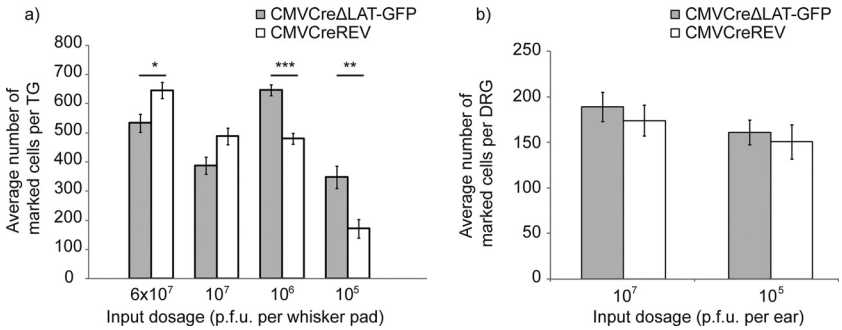

FIG 5 In the absence of LAT expression, the frequency of latency establishment is enhanced at "low" doses but diminishes at increasing doses. (a) R26R mice were infected on both whisker pads at a range of doses (10^5 to 6×10^7 PFU) and TG dissected ~30 d.p.i. for marked-cell quantification. Histograms represent the mean (± SEM) number of positive cells per ganglion at each dose. *P* values of <0.00005, <0.002, and 0.01 are represented by ***, **, and *, respectively. (b) R26R mice were infected on the left ear at 10^5 or 10^7 PFU doses. CII, III, and IV DRG were dissected 30 d.p.i. for marked-cell quantification. Histograms represent the mean (± SEM) number of positive cells per ganglion at each dose.

TG per day (Fig. 6a). Of note, while decreases in the sizes of the latent cell populations were consistently observed during LAT-negative infection, statistical significance was not achieved within individual experiments. However, statistical analysis of aggregate data from infections 29 to 30 d.p.i. and 135 to 140 d.p.i. (Table 2) determined the loss of cells during HSV CMVCreΔLAT-GFP infection to be significant ($P = 0.02$). HSV CMVCreREV marked-cell populations did not change significantly ($P = 0.28$). These data suggest that LAT-positive virus latency is largely stable, with an average loss of 0.11 ± 0.40 marked neurons per TG per day in comparison to the 1.66 ± 0.35 marked neurons lost per TG per day during LAT-negative virus latency (Fig. 6a). While LAT expression can be observed to maintain the stability of the latently infected cell reservoir, it is not clear how this is accomplished. To ascertain whether an increased level of spontaneous reactivation occurs in the ROSA26R mouse in the absence of LAT expression, latently infected TG were dissected, fixed, and processed for whole-mount detection of lytic antigen-positive neurons. Utilizing an anti-HSV polyclonal antibody, we were able to detect very low levels of lytic gene-positive cells at 44, 60, 66, and 69 d.p.i. From all time points, a total of six, three, and four positive cells were detected in TG infected with HSV CMVCre ($n = 40$ TG), HSV CMVCreΔLAT-GFP ($n = 44$ TG), and HSV CMVCreREV ($n = 46$ TG), respectively (Fig. 6b). TG positive for HSV-1 antigen typically contained just one HRP-labeled cell and could be detected from 20-μm-thick sections (Fig. 6b, panel ii) and from whole mounted ganglia (Fig. 6b, panel iii). These data are consistent with previous estimates of spontaneous reactivation with the mouse TG (23). These data indicate that spontaneous reactivation within the mouse TG is not dependent on LAT expression. With regard to maintenance, we observed that the mechanism of LAT-negative HSV-1-infected cell loss throughout latency does not operate via an increase in spontaneous reactivation, as measured using a polyclonal antibody. These data suggest that infected cells may be lost via apoptosis throughout latency, and such a mechanism clearly warrants further investigation.

TABLE 2 Summary of individual experimental data from maintenance study

Expt and strain	Avg (range) no. of marked cells per TG at the indicated time point			
	Early	Late	n^a	P^b
1	33 d.p.i.	110 d.p.i.		
HSV CMVCre	490 (244–639)	471 (223–714)	8–10	0.76
HSV CMVCreΔLAT	762 (506–1,028)	630 (303–885)	10	0.13
HSV CMVCreREV	543 (321–935)	455 (173–719)	10	0.41
2	30 d.p.i.	135 d.p.i.		
HSV CMVCreΔLAT-GFP	715 (270–1,105)	480 (88–843)	10	0.14
HSV CMVCreREV	564 (334–840)	587 (245–857)	10	0.65
3	29 d.p.i.	140 d.p.i.		
HSV CMVCreΔLAT-GFP	595 (271–1,009)	481 (214–783)	18–20	0.06
HSV CMVCreREV	423 (213–617)	503 (260–756)	18	0.16

[a] Numbers of ganglia enumerated per virus-infected group.
[b] *P* values obtained using Mann-Whitney U test.

DISCUSSION

In this paper, we have utilized the ROSA26R reporter mouse model in conjunction with Cre recombinase-expressing HSV-1 recombinants to investigate the role of LATs in the establishment and maintenance of neuronal infection latency. Previous studies have established that expression of Cre recombinase under the control of the HCMV MIEP results in the stable and efficient marking of latently infected neurons (29, 30, 47). This system therefore provides an amenable approach allowing direct measurement of the frequency of latently infected cells *in vivo*.

Previous studies have determined the frequency of latently infected neurons following infection of scarified corneas with 2×10^5 PFU of HSV-1, a procedure that results in 10% to 20% mortality of infected mice (42). Using this infection model, it has been shown that the HSV-1 strain KOS LATs are required for the efficient establishment of latency (44). Of importance, in this model system analysis at the single-neuron level has revealed that LAT-negative mutants establish only one-third as many latent infections as wild-type virus (44). Utilizing ROSA26R reporter mice, we report that, following low-dose ($\leq 10^6$ PFU) whisker pad infection with HSV-1 strain SC16 LAT-deficient viruses, an increased frequency of latency was observed relative to wild-type or revertant viruses. We define doses of $\leq 10^6$ PFU as "low" doses due to the observation that, following whisker pad inoculation with 10^4 PFU, we were unable to efficiently infect the ROSA26R TG (data not shown). Further, we were able to manipulate the relative

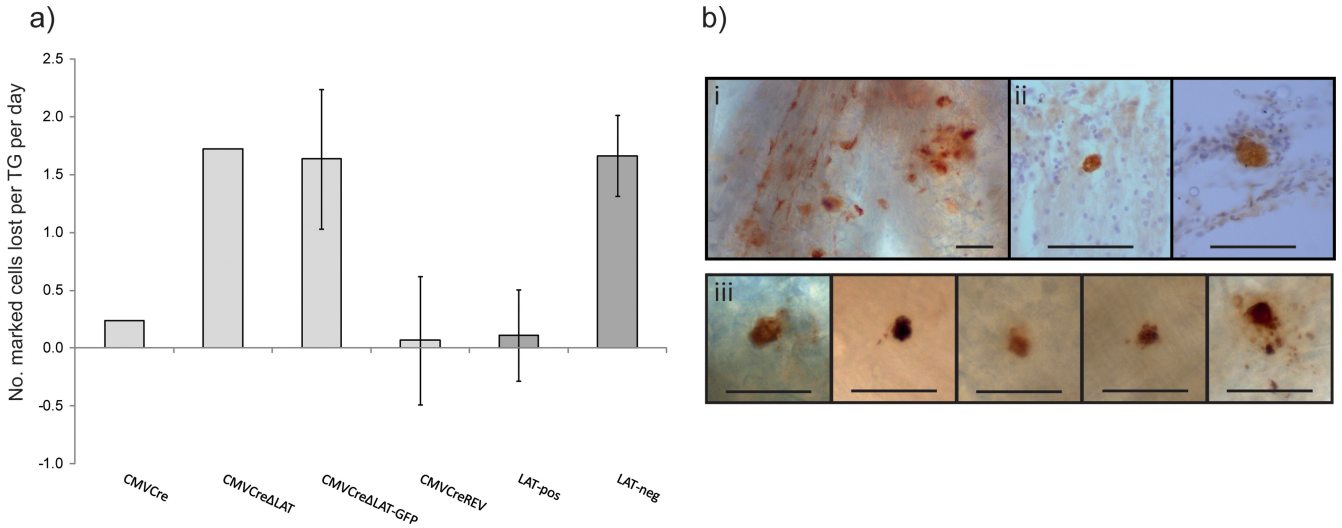

FIG 6 Maintenance of the latent cell reservoir is unstable in the absence of LAT expression. (a) R26R mice were infected on both whisker pads with 10^6 PFU and TG dissected at latency (29 to 33 d.p.i.) and "late" latency (110 to 140 d.p.i.) for marked-cell quantification. Histograms represent the mean number of marked cells lost per TG per day ± SEM. "LAT-pos" denotes both HSV CMVCre and HSV CMVCreREV data. "LAT-neg" denotes both HSV CMVCreΔLAT and HSV CMVCreΔLAT-GFP data. (b) Light micrographs of HSV-1 antigen-positive cells as detected via whole-ganglion immunohistochemistry. An example of acute infection within the TG at 4 d.p.i. is displayed in panel i. Panel ii displays antigen-positive cells detected in 20-μm-thick sections of latently infected TG at 44 d.p.i. Panel iii displays examples of antigen-positive cells detected at 44 d.p.i. to 69 d.p.i. All bars represent 100 μm.

efficiencies of establishment of infections by LAT-positive and LAT-negative viruses by altering the inoculum dose. Starting at an inoculum dose of 10^6 PFU, we observed that LAT-positive virus established latency at a reduced frequency, with just 75% of the number of neurons in which latency was established by LAT-negative virus. Dropping the inoculum dose to 10^5 PFU further exacerbated this difference, to between 33% to 62% of the total LAT-negative latent population. Conversely, increasing the inoculum dose beyond 10^6 PFU led to a loss of this phenotype, with LAT-positive virus establishing latency in 1.21 to 1.26 times as many neurons as LAT-negative virus. Though not similar in magnitude, the latter establishment phenotype is more consistent with previously reported data (44).

Taken together, these data suggest that the latency establishment phenotypes of HSV-1 mutants in the presence and absence of LAT expression are highly sensitive to the infection methodology, a fact that may confound absolute interpretation of LAT function *in vivo*. Despite the loss of the low-dose phenotype at increasing amounts of inoculum virus, we were unable to recapitulate previously reported data demonstrating severely reduced establishment efficiency in the absence of LAT expression (44). HSV-1 strains of higher virulence, different LAT mutations, greater infection doses (or at least more efficient infection methodologies), and differing inoculation sites may account for such observations. Despite such variables, a dose-dependent effect upon establishment may be a general feature of mouse infection and it is likely that these variables would simply affect the range of doses at which this is evident.

Previous studies have investigated the role of the inoculum dose in latency establishment following infection with wild-type HSV-1 and LAT-deficient mutants. A study utilizing the rabbit corneal model of infection found no difference in latent viral DNA loads in the TG at doses of 500 and 50,000 PFU (26). We have found that estimates of total latent viral DNA loads are a relatively insensitive measure by which to evaluate establishment efficiency. Thus, we have been unable to detect a statistically significant difference between wild-type and LAT-deficient mutants in total latent DNA loads ($P > 0.37$) despite a 30% increase in latent cell numbers following infection of reporter mice with a LAT-deficient mutant. Our inability to detect a statistically significant difference between LAT-positive and LAT-negative virus in total latent virus DNA loads is consistent with a number of previous studies with HSV-1 (3, 12, 28) and HSV-2 (18, 48, 49). In contrast, Hoshino et al. (13) demonstrated in 2009 that an HSV-2 (strain 333) LAT promoter mutant displayed a clear dose dependence during latency establishment within mouse TG but that, at the lowest doses employed, the latent DNA load of a LAT-null virus was lower than that of the corresponding revertant virus. Whether the reduced establishment of latency observed following low-dose HSV-2 infection relates to differences in the function of the HSV-1 and HSV-2 LATs or to virus strain and/or animal model differences is currently unclear. In our study, dose-dependent effects on establishment were observed within the TG but not the DRG, suggesting that, in addition to virus strain and/or animal model differences, the anatomical site of latency can impact virus mutant phenotypes.

We have been unable to observe increased titers during acute infection of the mouse with LAT-negative viruses and yet have observed increased numbers of marked cells at latency. Ongoing studies in our laboratory utilizing a fluorescent reporter mouse strain, allowing specific analysis of live marked cells, have determined that HSV-1 DNA is detectable only within the marked-cell population (unpublished observations). As such, increased neuronal cell marking by LAT-deficient mutants represents Cre recombinase-mediated reporter gene activation as a consequence of infection rather than a bystander effect. However, at this time, we cannot determine the LAT mechanism that results in this anatomically distinct and dose-dependent establishment phenotype.

HSV-1 LATs have multiple functions that include repression of viral IE gene expression (5, 10, 22, 37, 45), inhibition of apoptosis/promotion of cell survival (1, 4, 14, 27, 42), and regulation of histone-mediated repression of the HSV-1 genome during latency (6, 19, 50). Given these functions, it would perhaps be predicted that at low doses of infection, removal of LAT-mediated IE gene repression would favor lytic cycle entry in primarily infected neurons and increased spread within ganglionic tissue. In contrast, at high input doses, if LAT-mediated effects mitigating apoptosis were not present, a high proportion of primarily infected neurons might be killed without supporting virus replication, thus limiting virus spread through the tissue. While we were not able to detect increased replication efficiency of HSV CMVCreΔLAT-GFP within the TG following whisker pad infection (Fig. 2), the experiments may have been of insufficient statistical power to observe the presumably minor increase in replication titers needed to establish latency in ~33% more cells. However, this predicted "changing dominance" of LAT functions at low and high doses of viruses presents an appealing interpretation of our data and requires further investigation.

In this study, we also provide evidence for a role of LAT in maintaining latent infection of the mouse TG. By enumerating the number of marked cells in the ROSA26R TG at "early" (29 to 33 d.p.i.) and "long-term" (110 to 140 d.p.i.) times during latency, we consistently observed reductions in marked-cell populations during LAT-negative virus but not LAT-positive infection. These data suggest that LATs actively play a role in the maintenance of the latent cell reservoir. An assumption made in the interpretation of our current data is that the distribution of latency among distinct neuronal subpopulations is equivalent to that following wild-type virus infection. However, further work is necessary to define the neuronal populations latently infected by both LAT-deficient and wild-type viruses to investigate the possibility that mutant viruses establish latency in a neuronal population in which latency is intrinsically less stable.

By utilizing a previously described methodology for the detection of antigen-positive cells in whole-mount TG samples (33), we investigated whether the loss of marked cells was due to an increase in spontaneous reactivation during LAT-negative infection. However, upon interrogation of latently infected tissue, we found that antigen-positive cells could be detected at similarly low levels per ganglion for all viruses. These findings are consistent with earlier reports (23) and together suggest that LAT is not essential for spontaneous reactivation within the mouse TG. It is clear that the observed loss of marked cells during ROSA26R latency is not a result of increased spontaneous reactivation, as assessed by virus detection with an anti-HSV-1 polyclonal antibody. Whether this cell loss is due to an elevated frequency of apoptosis, possibly in response to the earliest stages of reactivation, is under investigation.

Previous investigations of HSV-1 latency maintenance have relied upon the assessment of total viral DNA within infected tissues (9, 11, 36). However, those studies do not provide a direct insight into the number of latently infected cells. With regard to the nonuniformity of viral DNA copy numbers per cell (32), it is thus currently unclear whether a loss of infected cells would manifest in a proportional loss of total viral DNA within the ganglion. A previous study (17) revealed that disruption of splicing of the primary LAT resulted in an approximately 10-fold reduction in the latent genome copy number in mouse TG. However, due to the assessment of a single latent time point, it was not possible to discern whether the observed phenotype was due to a deficit in the establishment or maintenance of latency.

Of great interest, a recent report determined that, following repeated induction of *in vivo* reactivation by hyperthermic stress, a LAT-negative virus suffered a reduced capacity to reactivate between 30 days and 42 weeks postinfection (43). These data are consistent with our findings, as a loss of infected cells over a prolonged period of time could be hypothesized to reduce reactivation frequency within the TG. While we did not observe a difference in spontaneous reactivation frequency (as measured by HSV-1 lytic antigen-positive cell numbers), our analyses were conducted both earlier and without reactivation stimuli. Therefore, a larger reduction in the latent cell population may be required to observe a reactivation deficit.

It is important that all viruses utilized within this study were constructed by replacing the viral U_S5 gene with a Cre recombinase expression cassette. This mutation removes expression of glycoprotein J (gJ), a protein of known antiapoptosis function (16), and may thus sensitize the recombinants in this study to the effects of apoptosis. Nonetheless, we observed no effect upon the *in vivo* replication kinetics in comparisons of gJ-deficient LAT-positive and LAT-negative viruses. In addition, stable maintenance of latency was observed during infection with gJ-deficient LAT-positive viruses, indicating that gJ antiapoptotic functions play little or no role in latency. Studies of LAT-negative HSV-1 gene expression have shown elevated lytic transcript accumulation during latency (5), consistent with increased lytic gene expression during acute infection (10). In the context of LAT-deficient mutants, such "leaky" expression of genes in the lytic cycle could increase the probability of virus reactivation and/or the engagement of an apoptotic program that in the absence of LATs cannot be effectively curtailed.

In summary, our studies suggest that the HSV-1 latency-associated transcripts function to (i) enhance the efficiency of latency establishment following high-dose infection, (ii) reduce the efficiency of latency establishment following low-dose infection, and (iii) facilitate the long-term maintenance of the latent cell reservoir.

ACKNOWLEDGMENTS

This research was supported by the Wellcome Trust (project grant 086403/Z/08/7) and the Medical Research Council (MRC) UK (MR/J002232/1). M.N. is supported by an MRC (UK) Ph.D. studentship.

REFERENCES

1. **Ahmed M, Lock M, Miller CG, Fraser NW.** 2002. Regions of the herpes simplex virus type 1 latency-associated transcript that protect cells from apoptosis in vitro and protect neuronal cells in vivo. J. Virol. **76**:717–729.
2. **Arthur JL, Everett R, Brierley I, Efstathiou S.** 1998. Disruption of the 5′ and 3′ splice sites flanking the major latency-associated transcripts of herpes simplex virus type 1: evidence for alternate splicing in lytic and latent infections. J. Gen. Virol. **79**(Pt 1):107–116.
3. **Bloom DC, Devi-Rao GB, Hill JM, Stevens JG, Wagner EK.** 1994. Molecular analysis of herpes simplex virus type 1 during epinephrine-induced reactivation of latently infected rabbits in vivo. J. Virol. **68**:1283–1292.
4. **Branco FJ, Fraser NW.** 2005. Herpes simplex virus type 1 latency-associated transcript expression protects trigeminal ganglion neurons from apoptosis. J. Virol. **79**:9019–9025.
5. **Chen SH, Kramer MF, Schaffer PA, Coen DM.** 1997. A viral function represses accumulation of transcripts from productive-cycle genes in mouse ganglia latently infected with herpes simplex virus. J. Virol. **71**:5878–5884.
6. **Cliffe AR, Garber DA, Knipe DM.** 2009. Transcription of the herpes

simplex virus latency-associated transcript promotes the formation of facultative heterochromatin on lytic promoters. J. Virol. **83**:8182–8190.
7. **Coleman HM, et al.** 2008. Histone modifications associated with herpes simplex virus type 1 genomes during quiescence and following ICP0-mediated de-repression. J. Gen. Virol. **89**:68–77.
8. **Dush MK, Sikela JM, Khan SA, Tischfield JA, Stambrook PJ.** 1985. Nucleotide sequence and organization of the mouse adenine phosphoribosyltransferase gene: presence of a coding region common to animal and bacterial phosphoribosyltransferases that has a variable intron/exon arrangement. Proc. Natl. Acad. Sci. U. S. A. **82**:2731–2735.
9. **Efstathiou S, Minson AC, Field HJ, Anderson JR, Wildy P.** 1986. Detection of herpes simplex virus-specific DNA sequences in latently infected mice and in humans. J. Virol. **57**:446–455.
10. **Garber DA, Schaffer PA, Knipe DM.** 1997. A LAT-associated function reduces productive-cycle gene expression during acute infection of murine sensory neurons with herpes simplex virus type 1. J. Virol. **71**:5885–5893.
11. **Hill JM, et al.** 1996. Quantitation of herpes simplex virus type 1 DNA and latency-associated transcripts in rabbit trigeminal ganglia demonstrates a stable reservoir of viral nucleic acids during latency. J. Virol. **70**:3137–3141.
12. **Hill JM, Sedarati F, Javier RT, Wagner EK, Stevens JG.** 1990. Herpes simplex virus latent phase transcription facilitates in vivo reactivation. Virology **174**:117–125.
12a. **Hill TJ, Field HJ, Blyth WA.** 1975. Acute and recurrent infection with herpes simplex virus in the mouse: a model for studying latency and recurrent disease. J. Gen. Virol. **28**:341–353.
13. **Hoshino Y, Pesnicak L, Straus SE, Cohen JI.** 2009. Impairment in reactivation of a latency associated transcript (LAT)-deficient HSV-2 is not solely dependent on the latent viral load or the number of CD8(+) T cells infiltrating the ganglia. Virology **387**:193–199.
14. **Inman M, et al.** 2001. Region of herpes simplex virus type 1 latency-associated transcript sufficient for wild-type spontaneous reactivation promotes cell survival in tissue culture. J. Virol. **75**:3636–3646.
15. **Javier RT, Stevens JG, Dissette VB, Wagner EK.** 1988. A herpes simplex virus transcript abundant in latently infected neurons is dispensable for establishment of the latent state. Virology **166**:254–257.
16. **Jerome KR, et al.** 1999. Herpes simplex virus inhibits apoptosis through the action of two genes, Us5 and Us3. J. Virol. **73**:8950–8957.
17. **Kang W, Mukerjee R, Fraser NW.** 2003. Establishment and maintenance of HSV latent infection is mediated through correct splicing of the LAT primary transcript. Virology **312**:233–244.
18. **Krause PR, et al.** 1995. Expression of the herpes simplex virus type 2 latency-associated transcript enhances spontaneous reactivation of genital herpes in latently infected guinea pigs. J. Exp. Med. **181**:297–306.
19. **Kwiatkowski DL, Thompson HW, Bloom DC.** 2009. The polycomb group protein Bmi1 binds to the herpes simplex virus 1 latent genome and maintains repressive histone marks during latency. J. Virol. **83**:8173–8181.
20. **Lachmann RH, Efstathiou S.** 1997. Utilization of the herpes simplex virus type 1 latency-associated regulatory region to drive stable reporter gene expression in the nervous system. J. Virol. **71**:3197–3207.
21. **Leib DA, et al.** 1989. A deletion mutant of the latency-associated transcript of herpes simplex virus type 1 reactivates from the latent state with reduced frequency. J. Virol. **63**:2893–2900.
22. **Mador N, Goldenberg D, Cohen O, Panet A, Steiner I.** 1998. Herpes simplex virus type 1 latency-associated transcripts suppress viral replication and reduce immediate-early gene mRNA levels in a neuronal cell line. J. Virol. **72**:5067–5075.
23. **Margolis TP, et al.** 2007. Spontaneous reactivation of herpes simplex virus type 1 in latently infected murine sensory ganglia. J. Virol. **81**:11069–11074.
24. **McGeoch DJ, et al.** 1988. The complete DNA sequence of the long unique region in the genome of herpes simplex virus type 1. J. Gen. Virol. **69**(Pt 7):1531–1574.
25. **Nicoll MP, Proença JT, Efstathiou S.** 2012. The molecular basis of herpes simplex virus latency. FEMS Microbiol. Rev. **36**:684–705.
26. **O'Neil JE, et al.** 2004. Wide variations in herpes simplex virus type 1 inoculum dose and latency-associated transcript expression phenotype do not alter the establishment of latency in the rabbit eye model. J. Virol. **78**:5038–5044.
27. **Perng G-C, et al.** 2000. Virus-induced neuronal apoptosis blocked by the herpes simplex virus latency-associated transcript. Science **287**:1500–1503.
28. **Perng GC, et al.** 1994. The latency-associated transcript gene of herpes simplex virus type 1 (HSV-1) is required for efficient in vivo spontaneous reactivation of HSV-1 from latency. J. Virol. **68**:8045–8055.
29. **Proença JT, Coleman HM, Connor V, Winton DJ, Efstathiou S.** 2008. A historical analysis of herpes simplex virus promoter activation in vivo reveals distinct populations of latently infected neurones. J. Gen. Virol. **89**:2965–2974.
30. **Proença JT, et al.** 2011. An investigation of HSV promoter activity compatible with latency establishment reveals VP16 independent activation of HSV immediate early promoters in sensory neurones. J. Gen. Virol. **92**(Pt 11):2575–2585.
31. **Rock DL, et al.** 1987. Detection of latency-related viral RNAs in trigeminal ganglia of rabbits latently infected with herpes simplex virus type 1. J. Virol. **61**:3820–3826.
32. **Sawtell NM.** 1997. Comprehensive quantification of herpes simplex virus latency at the single-cell level. J. Virol. **71**:5423–5431.
33. **Sawtell NM.** 2003. Quantitative analysis of herpes simplex virus reactivation in vivo demonstrates that reactivation in the nervous system is not inhibited at early times postinoculation. J. Virol. **77**:4127–4138.
34. **Sawtell NM, Poon DK, Tansky CS, Thompson RL.** 1998. The latent herpes simplex virus type 1 genome copy number in individual neurons is virus strain specific and correlates with reactivation. J. Virol. **72**:5343–5350.
35. **Sawtell NM, Thompson RL.** 1992. Herpes simplex virus type 1 latency-associated transcription unit promotes anatomical site-dependent establishment and reactivation from latency. J. Virol. **66**:2157–2169.
36. **Sedarati F, Izumi KM, Wagner EK, Stevens JG.** 1989. Herpes simplex virus type 1 latency-associated transcription plays no role in establishment or maintenance of a latent infection in murine sensory neurons. J. Virol. **63**:4455–4458.
37. **Shen W, et al.** 2009. Two small RNAs encoded within the first 1.5 kilobases of the herpes simplex virus type 1 latency-associated transcript can inhibit productive infection and cooperate to inhibit apoptosis. J. Virol. **83**:9131–9139.
38. **Soares K, et al.** 1996. cis-acting elements involved in transcriptional regulation of the herpes simplex virus type 1 latency-associated promoter 1 (LAP1) in vitro and in vivo. J. Virol. **70**:5384–5394.
39. **Soriano P.** 1999. Generalized lacZ expression with the ROSA26 Cre reporter strain. Nat. Genet. **21**:70–71.
40. **Steiner I, et al.** 1989. Herpes simplex virus type 1 latency-associated transcripts are evidently not essential for latent infection. EMBO J. **8**:505–511.
41. **Stevens JG, Wagner EK, Devi-Rao GB, Cook ML, Feldman LT.** 1987. RNA complementary to a herpesvirus alpha gene mRNA is prominent in latently infected neurons. Science **235**:1056–1059.
42. **Thompson RL, Sawtell NM.** 2001. Herpes simplex virus type 1 latency-associated transcript gene promotes neuronal survival. J. Virol. **75**:6660–6675.
43. **Thompson RL, Sawtell NM.** 2011. The herpes simplex virus type 1 latency associated transcript locus is required for the maintenance of reactivation competent latent infections. J. Neurovirol. **17**:552–558.
44. **Thompson RL, Sawtell NM.** 1997. The herpes simplex virus type 1 latency-associated transcript gene regulates the establishment of latency. J. Virol. **71**:5432–5440.
45. **Umbach JL, et al.** 2008. MicroRNAs expressed by herpes simplex virus 1 during latent infection regulate viral mRNAs. Nature **454**:780–783.
46. **Wagner EK, Bloom DC.** 1997. Experimental investigation of herpes simplex virus latency. Clin. Microbiol. Rev. **10**:419–443.
47. **Wakim LM, Jones CM, Gebhardt T, Preston CM, Carbone FR.** 2008. CD8(+) T-cell attenuation of cutaneous herpes simplex virus infection reduces the average viral copy number of the ensuing latent infection. Immunol. Cell Biol. **86**:666–675.
48. **Wang K, Pesnicak L, Guancial E, Krause PR, Straus SE.** 2001. The 2.2-kilobase latency-associated transcript of herpes simplex virus type 2 does not modulate viral replication, reactivation, or establishment of latency in transgenic mice. J. Virol. **75**:8166–8172.
49. **Wang K, Pesnicak L, Straus SE.** 1997. Mutations in the 5′ end of the herpes simplex virus type 2 latency-associated transcript (LAT) promoter affect LAT expression in vivo but not the rate of spontaneous reactivation of genital herpes. J. Virol. **71**:7903–7910.
50. **Wang Q-Y, et al.** 2005. Herpesviral latency-associated transcript gene promotes assembly of heterochromatin on viral lytic-gene promoters in latent infection. Proc. Natl. Acad. Sci. U. S. A. **102**:16055–16059.